Editors' Suggestion

Collective Charge Excitations between Moiré Minibands in Twisted WSe_2 Bilayers Probed with Resonant Inelastic Light Scattering

Nihit Saigal,[1] Lennart Klebl,[2] Hendrik Lambers,[1] Sina Bahmanyar,[1] Veljko Antić,[1] Dante M. Kennes,[3,4] Tim O. Wehling,[2,5] and Ursula Wurstbauer[1,6,*]

[1]*Institute of Physics, University of Münster, Wilhelm-Klemm-Strasse 10, 48149 Münster, Germany*
[2]*Institute of Theoretical Physics, University of Hamburg, Notkestrasse 9, 22607 Hamburg, Germany*
[3]*Institute for Theory of Statistical Physics, RWTH Aachen University, and JARA Fundamentals of Future Information Technology, 52062 Aachen, Germany*
[4]*Max Planck Institute for the Structure and Dynamics of Matter, Center for Free Electron Laser Science, 22761 Hamburg, Germany*
[5]*The Hamburg Centre for Ultrafast Imaging, 22761 Hamburg, Germany*
[6]*Center for Soft Nanoscience (SoN), Busso-Peus-Strasse 10, 48149 Münster, Germany*

(Received 31 October 2023; revised 13 April 2024; accepted 7 June 2024; published 23 July 2024)

We establish low-temperature resonant inelastic light scattering (RILS) spectroscopy as a tool to probe the formation of a series of moiré bands in twisted WSe_2 bilayers by accessing collective inter-moiré-band excitations (IMBEs). We observe resonances in RILS spectra at energies in agreement with inter-moiré-band transitions obtained from an *ab initio* based continuum model. Transitions between the first and second moiré band for a twist angle of about 8° are reported and between the first and the third, and higher bands for a twist of about 3°. The signatures from IMBE for the latter highlight a strong departure from parabolic bands with flat minibands exhibiting very high density of states in accord with theory. These observations allow one to quantify the transition energies at the K point where the states relevant for correlation physics are hosted.

DOI: 10.1103/PhysRevLett.133.046902

Twisted van der Waals (vdW) bilayers present a unique condensed matter platform to realize and control electronic correlation effects [1–3]. The large scale superlattice created by the superposition of the two layers at a slight rotational mismatch defines a reciprocal mini-Brillouin zone with nearly dispersionless (flat) bands as long as the layers hybridize sufficiently. The drastically reduced kinetic energy results in a very high density of states (DOS) and even Van Hove physics in those bands, driving electrons into the correlated regime [4,5]. In several graphene-based systems correlated and ordered electronic phases are experimentally well established [6–10]. In transition metal dichalcogenide- (TMDC) based vdW stacks, the absence of complications like topological obstructions have facilitated high-level microscopic many-body studies from early on [11] and explained the emergence of ordered, insulating, and also different flavors of correlated metallic states of matter [12,13]. Experimentally, the aforementioned correlation effects have been realized [14,15], while superconductivity has remained elusive with currently one report of an (unclear and controversial) zero resistance state [14], even though there are multiple theoretical studies [16–18].

These emergent phases in semiconductor-based moiré bilayers are attributed to strongly interacting electronic K/K' states. In this Letter, we experimentally access moiré minibands at the valence band maximum (VBM) around the K/K' valley by studying their collective electronic inter-moiré-band excitations (IMBEs) by resonant inelastic light scattering (RILS) experiments as summarized in Fig. 1. Accessing the moiré bands at the K points is challenging for the combined reason of twist angle variations and reconstruction in realistic devices together with the VBM at the Γ and K points being close in energy [19]. The morphology of twisted bilayers, particularly at small twist angles, is such that variations in twist angle, but also reconstruction (in plane as well as corrugation) plays an important role. This leads to periodically patterned areas different from those expected from a rigid moiré lattice picture [20–23]. While these patterns result in rich optical interband spectra [23] and even host coherent many-body states of excitons [24], it makes the interpretation of spectroscopic signatures and the direct spectroscopy of moiré bands, e.g., by angle-resolved photoemission spectroscopy (ARPES) difficult with only a few reports on selected material combinations [25,26]. Recent μ-ARPES and STM studies demonstrate the formation of moiré bands at the VBM at the Γ point of twisted WSe_2 bilayers [22,27,28]. Accessing moiré bands around the K/K' states and their properties is still lacking.

We remedy this standing problem by reporting on collective electronic excitations between moiré bands formed in

*Contact author: wurstbauer@uni-muenster.de

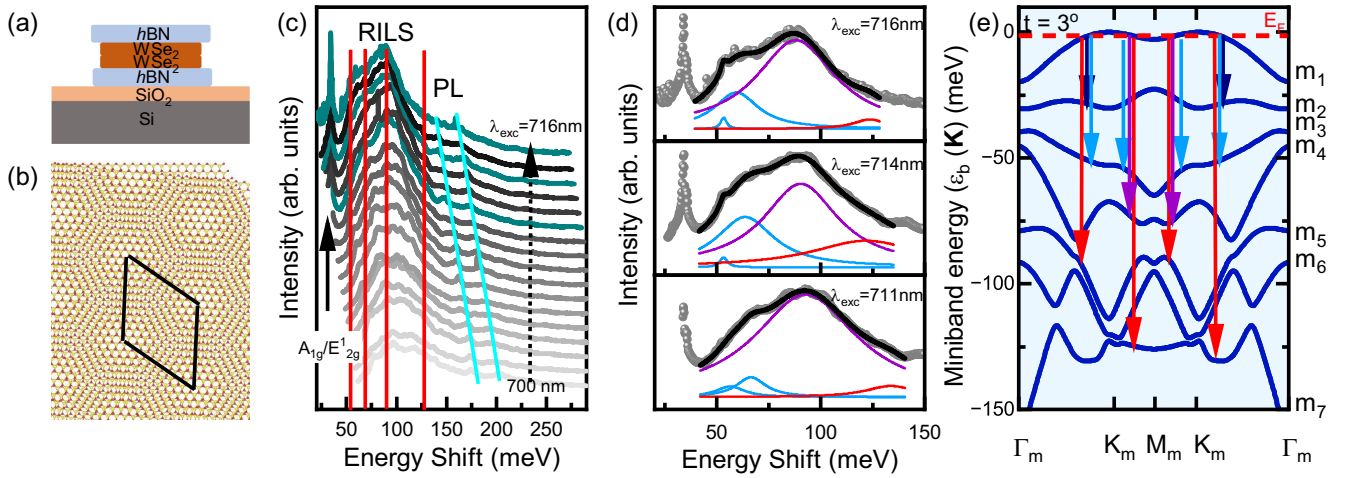

FIG. 1. (a) Scheme of the h-BN encapsulated $tWSe_2$ bilayer. (b) Stick-ball model of a moiré superlattice from a $tWSe_2$ bilayer with the moiré unit cell indicated. (c) RILS spectra on a 3° $tWSe_2$ bilayer. Spectra are offset for clarity. The A_{1g}/E^1_{2g} phonons are indicated by a black solid arrow. The broad RILS signals are collective electronic IMBEs. The vertical red solid lines mark resonance energies from theoretically predicted transition energies. The tilted cyan lines indicate emission signatures. For the dark cyan spectra results from line shape analysis are shown in (d) ($T = 4$ K, $P_{\mathrm{Laser}} = 1$ mW). (d) Selected RILS spectra (data points) from (c). The solid lines are fit results, using a set of Lorentzian lines to numerically deconvolute the individual contribution from the RILS spectra. The black lines are the sum of all Lorentzian curves. (e) Calculated energy dispersion of the seven highest moiré minibands around the K, K' states for a 3° $tWSe_2$ bilayer. The minibands are labeled $m_1, m_2, \ldots, m_7$. Exemplary interminiband transitions are sketched.

twisted and h-BN encapsulated WSe_2 bilayers [Figs. 1(a) and 1(b)] at the VBM around the K/K' states. By combined theoretical and experimental efforts, we demonstrate that probing the moiré bands via collective single-particle-like IMBE by RILS spectroscopy analog to intersubband excitations in 2D charge carrier systems hosted, e.g., in GaAs quantum wells [29–31] provides a promising approach to study the band structure of twisted transition metal dichalcogenides at twist angles where correlation physics plays an important role [3,12,13,16–18].

The h-BN encapsulated $tWSe_2$ bilayers have been prepared by micromechanical cleavage and viscoelastic dry transfer on top of Si/SiO_2 substrates with an estimated twist uncertainty of about ±0.5°. Three different types of WSe_2 samples have been prepared with a twist of 3°, 8°, and a natural homobilayer. To check for sufficient interlayer coupling and twist angle we employ low-temperature nonresonant Raman and PL spectroscopy (see Supplemental Material, Figs. 1 and 2 [32]). For all measurements, the samples are mounted on the cold finger of a closed-cycle refrigerator at a temperature of $T = 4$ K if not stated otherwise. Position control is provided by x-y-z piezoactuators. The light from either a green solid state laser (2.33 eV) or a continuously tunable Ti:sapphire laser (linewidth of about 50 kHz) is focused with a cryogenic large-NA (NA = 0.82) objective lens to spot size of less than 2 μm. The emitted and/or scattered light is guided to the entrance slit of a triple grating spectrometer. In RILS experiments, the sample is excited by linearly polarized light in backscattering geometry and the scattered light is unpolarized (see Supplemental Material, Fig. 6 for polarization-dependent spectra [32]). Because of the large NA of the objective a distribution of in-plane momenta $q_{\parallel} < 2\omega_{\mathrm{L}}/c \sin\theta_{\max}$ with $\theta_{\max} \approx 55°$ is transferred to the hole system.

By excitation in resonance close to the direct optical allowed interband transition at the K/K' point (A_{1s} exciton), IMBEs at the K/K' VBM can be probed by low-temperature RILS spectroscopy. Typical RILS spectra taken on a $t \approx 3°$ twisted WSe_2 bilayer at $T = 4$ K are shown in a waterfall representation in Fig. 1(c). The resonance excitation wavelengths are determined from PL experiments (see Supplemental Material, Fig. 1 [32]). A rich spectrum of rather wide and dispersive RILS modes (red lines) is accompanied by the sharp nearly degenerate optical active A_{1g}, E^1_{2g} phonon modes at an energy range between 20 and 120 meV. In order to deconvolute individual contributions to the RILS spectra, we perform a line shape analysis by fitting a sum of Lorentzian curves to the spectra. We first focus on the energy range between 40 and 130 meV. The RILS spectra for all excitation wavelengths used are well reproduced by a sum of four (five) Lorentz functions for larger and smaller wavelengths, respectively. The energetic positions of the individual terms stay nearly constant, while the intensities are affected by the resonance conditions. This finding strongly suggests that the observed RILS mode originates from scattering on collective electronic excitation in analogy to intersubband excitations in GaAs-based low-dimensional structures [29,36,37]. We would like to note that the quantitative interpretation from a similar quantitative line shape analysis in the 20–35 meV range is challenging since at least seven phonon modes under the chosen resonance conditions are reported in

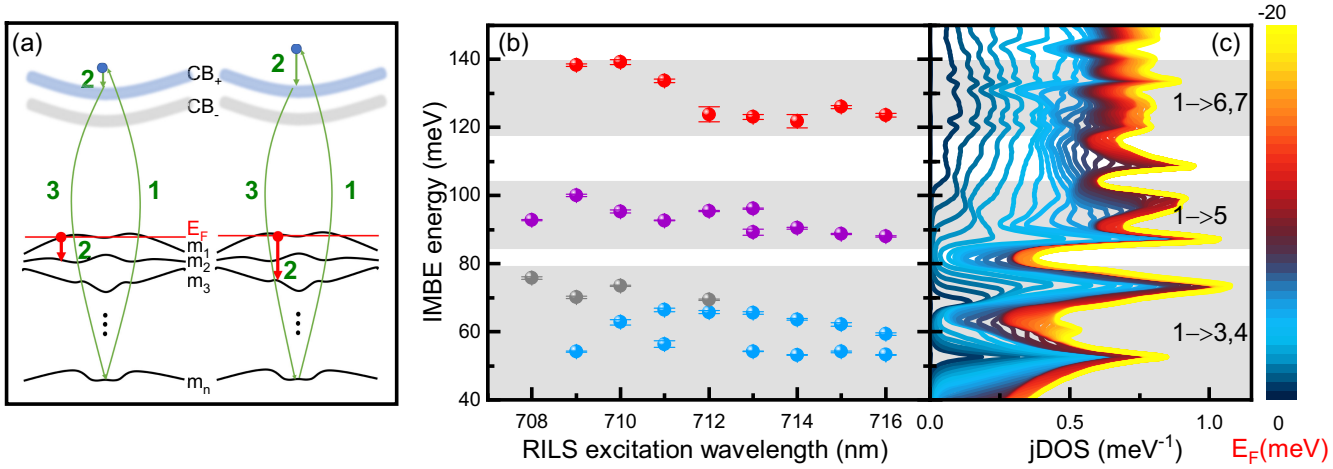

FIG. 2. (a) Schematic picture of the three-step scattering process for creation of IMBE between moiré minibands formed in the valence band (VB) around the K points. In the first step, an electron is excited from a lower VB to a virtual state; in the second step, the charge carrier is scattered by Coulomb interaction with photoexcited hole from m_1 to m_2 (left) and from m_1 to m_3 (right) under creation of an IMBE. In the third step, the electron recombines. (b) Extracted peak energies from the line shape analysis described in Fig. 1 for 3° $tWSe_2$. (c) Calculated jDOS for interminiband transitions in dependence of the Fermi-level E_F (color coded) of 3° $tWSe_2$ for vertical transitions. The peaks of the theoretical jDOS calculation are in good agreement with the Lorentzian fits to the experimental data (b).

literature [38]. Superimposed to these phonon modes and PL background, an additional mode occurs under extreme resonance at the red of the tail A_{1g}, E^1_{2g} phonon modes at an energy of about 28.8 meV (for a detailed analysis, see Supplemental Material, Fig. 5 [32]). Because of its occurrence only under extreme resonance, in contrast to the resonantly activated phonon modes, we assign this mode also to an electronic excitation.

The extracted mode energies are in good quantitative agreement with inter-moiré-band transitions extracted from the calculated electronic bands in the mini-Brillouin-zone (mBZ) in the vicinity of the K/K' points. For direct comparison, Fig. 1(e) summarizes the first seven moiré minibands with examples of vertical transitions starting from the Fermi surface in the highest moiré band m_1. We obtain the band structures of $tWSe_2$ from a continuum model [3,39–41] with parameters adjusted to *ab initio* simulations (for details see Supplemental Material [32]).

We explain the observed RILS spectra by a three-step scattering process for IMBE of photogenerated holes following the concept well established for single-particle intersubband excitations in GaAs-based films [29–31] and successfully applied to, e.g., RILS on intersubband excitation of photogenerated electrons and holes in ultrathin GaAs-based nanowires [37]. Figure 2(a) illustrates the scattering processes for the $m_1 \rightarrow m_2$ (left) and $m_1 \rightarrow m_3$ (right) transitions: In the first step, an electron from a valence band (VB) state at K/K' is excited to a virtual state close to the upper conduction band (CB) at K/K' (spin allowed transition). If the virtual electronic state is just above the CB by the energy of an IMBE, in the second step, the electron can be resonantly scattered via Coulomb interaction with a hole in m_1 miniband at the (quasi) Fermi level to the CB. Simultaneously, an IMBE (e.g., $m_1 \rightarrow m_2$) is created in the valence band. In the third step, the scattered electron-hole pair recombines under emission of the scattered photon. The same concept applies by including excitonic effects (not included in the scheme for clarity). The experiment is done under cw excitation such that a plasma of photogenerated holes is forming a quasi-Fermi-level in the topmost miniband due to quick relaxation. We assume a charge imbalance between electrons and holes at the K/K' valley since the WSe_2 is expected to be slightly hole doped and, in addition, photogenerated electrons are supposed to relax into the energetically lower Σ valley [42].

Since the joint density of states (jDOS) is dependent on E_F, complementary excitation power-dependent RILS measurements are done in order to vary E_F by the photoinduced holes from $\Delta p \approx 10^9$ to $\Delta p \approx 10^{10}$ and $\Delta p \approx 10^{12}$ cm^{-2}. Because of the strong band nonparabolicity and the unknown intrinsic doping, it was not possible to estimate the change in E_F from Δp. In agreement with expectation from jDOS, the RILS intensities in the lower-energy region assigned to superimposed phonons and collective electronic excitations including the tentative IMBE $m_1 \rightarrow m_2$ is reduced, while the modes are enhanced with slight modification in their energies in line with expectations from theory (spectra and summary from line shape analysis shown in Supplemental Material, Figs. 3 and 4 [32]).

In Fig. 2(b) we summarize IMBE energies extracted from the line shape analysis of the RILS spectra of the 3° $tWSe_2$ described above. The nominal numerical fit error

is only a few percent. The partially ascending slopes for few data points in dependence of the excitation wavelength is assigned to superimposed PL. The mode energies are directly compared to the calculated jDOS of the individual transitions displayed in Fig. 2(c) in dependence of the position of E_F (color code) demonstrating its significant E_F dependency. Mode energies and the jDOS are in good quantitative agreement assuming a realistic Fermi energy of less than a few meV. In the energy range between 50 and 80 meV, two well-separated modes can be identified that are assigned to two $m_1 \rightarrow m_3$ transitions and one $m_1 \rightarrow m_4$ transition; the third one might be another $m_1 \rightarrow m_3$ superimposed by PL. The mode observed at an energy of about 95 meV is assigned to the $m_1 \rightarrow m_5$ transition and the modes observed around 123 and 140 meV to $m_1 \rightarrow m_6$ and $m_1 \rightarrow m_7$ and higher transitions, respectively. Minor deviation between theory and experiment can have the following concurrent origins: (i) The moiré bands are flat but still dispersing in a highly nonparabolic manner such that they themselves have a finite width of up to a few tens of meV with overlapping bands, particularly for m_3 and higher. (ii) Nonvertical transitions between points with a high DOS are expected to contribute to finite momentum transfer $q_\parallel$ in addition to defect-induced breakdown of momentum conservation [43]. (iii) Twist angle variations of at least $\pm 0.3°$ within the laser spot have a crucial impact on the moiré band formation as discussed below.

We contrast RILS spectra in a false color representation taken on 3° $tWSe_2$ [Fig. 3(a)], natural bilayer (NBL) WSe_2 [Fig. 3(b)], and 8° $tWSe_2$ [Fig. 3(c)] for an extended range of excitation wavelengths. RILS intensities are encoded in the color scheme. In the RILS spectra of the twisted bilayers 3° $tWSe_2$ and 8° $tWSe_2$ displayed in Figs. 3(a) and 3(c), highly resonant, intense, and rather broad RILS modes interpreted as IMBE dominate the RILS spectra. In addition to the phonon and IMBE resonances, a few features occur with energies depending on the incoming laser energy (tiled white lines) that are interpreted as defect or 0D moiré potential localized emission signatures. The double resonance behavior with a splitting of 15 meV only observed for 3° is in agreement with reported splitting in absorption and emission spectra for lower twist angles [21].

For the NBL sample, despite the sharp phonon resonance, no clear RILS modes occur. The spectra are dominated by typical emission signatures. These lines are likely due to emission from interlayer excitons [19]. The absence of RILS modes for NBLs is expected due to the absence of moiré lattice and minibands. The energy separation of the SOI-split valence bands is on the order of a few hundreds of meV [44] and hence far beyond the investigated energy range. For the 8° $tWSe_2$, instead, one weaker and one dominant broad RILS resonance appear at an energy range of about 60–120 meV. In this energy range, a good fit to the RILS spectra is achieved by a sum of two Lorentzian terms [see example spectrum with fit overlaid in Fig. 3(c)]. For a quantitative comparison with theory, the related band structure for the moiré mBZ around the VBM at the K point is displayed in Fig. 3(d) in the experimentally relevant energy range (for extended range, see Supplemental Material, Fig. 7 [32]). For such a large twist, the bands are nearly parabolic with larger energy separation. In comparison with theory, the weaker RILS mode at ≈60 meV could be interpreted as a collective intraband transition within the m_1 band as sketched in Fig. 3(d). The more intense, broader RILS mode at ≈75–115 meV is interpreted as an IMBE $m_1 \rightarrow m_2$ transition with the broadening due to nonvertical transitions provided by the finite transferred in-plane momentum $q_\parallel \leq q_{\max}$. The good quantitative agreement justifies our interpretation of the modes as being collective intra- and interband excitations allowing one to study the band structure of the mBZ at the K points. In the following, we consider the impact of realistic twist angle variations to be on the order of $\pm 0.3°$. While it is shown from calculated bands to be negligibly small for $(8 \pm 0.5)°$ $tWSe_2$, the impact is significant in the miniband energies and dispersion for $(3 \pm 0.3)°$ $tWSe_2$ as plotted in Fig. 3(e). As highlighted above, twist angle variation together with nonvertical transitions and finite momentum transfer results in broadened IMBE signatures in RILS. The RILS modes are a convolution of jDOS and the momentum distribution. We would like to note that we do not observe sizable differences for linear co- and linear cross-polarization in the RILS spectra (see Supplemental Material, Fig. 6 [32]). This finding supports our interpretation that the RILS modes are a single-particle type of IMBE rather than plasmalike charge- or spin-density excitations that show both a distinct polarization dependence [37]. To further substantiate our interpretation, we perform temperature-dependent RILS measurements [Fig. 3(f)]. To avoid heating effects, the excitation power is reduced to $P = 50$ μW and the excitation wavelength kept constant at extreme resonance condition at $\lambda = 710$ nm. The RILS signal shows a clear temperature dependence and is reduced with increasing temperature. Already at 10 K the RILS modes fade out and the PL background starts to dominate the spectrum. We observe similar reduction in RILS intensity with increasing temperature for the 8° $tWSe_2$ sample (see Supplemental Material, Fig. 6 [32]). All experimental observations together strongly support the interpretation that the observed broad RILS signatures are indeed collective IMBE between moiré bands at the VBM at the K/K' valley in excellent agreement to theory. We would like to emphasize that collective excitations probe the weakly disordered parts of the sample, while disorder often results in the most dominant signatures in emission experiments due to rather bright localized emission and disturbs transport investigations by additional scattering channels.

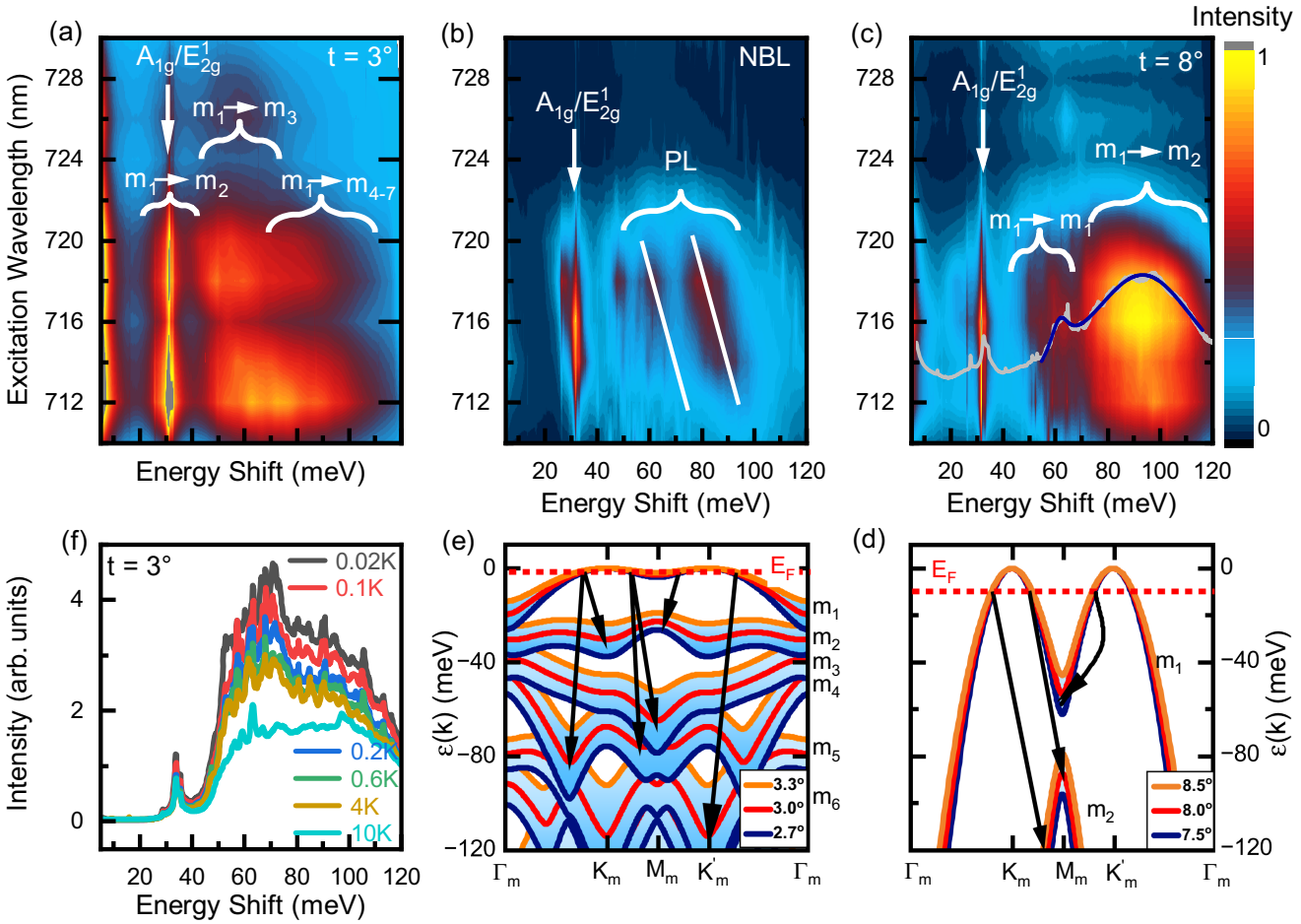

FIG. 3. RILS spectra on (a) 3° $tWSe_2$, (b) natural bilayer WSe_2, and (c) 8° $tWSe_2$. The straight white arrows indicate phonon modes and the white curly braces in (a) and (c) IMBE with moiré band assignment according to calculations. In the natural bilayer spectra (b) in addition to the vertical phonon line only shifting emission signals marked with tilted white lines emerge. In (c) an individual spectrum is exemplarily overlaid in gray color with a fit to the data (blue line) using the sum of two Lorentz curves ($T = 4$ K, $P_{\text{laser}} = 500$ μW; inset: $\lambda_{\text{laser}} = 712$ nm). (d) Calculated electronic band structure for $(8 \pm 0.5)°$ considering realistic twist variations. (e) Calculated electronic band structure for $(3 \pm 0.3)°$. Twist variations can result in broadened minibands causing significantly broadened IMBE in RILS experiments. Breakdown of wave vector conservation together with finite transferred in-plane momentum $q_{\parallel}$ due to the high NA of the objective allows also for nonvertical transitions to points of the minibands with high DOS as indicated by the arrows. (f) Temperature-dependent RILS spectra for $10 < T < 10$ K for 3° $tWSe_2$ ($\lambda_{\text{exc}} = 710$ nm, $P_{\text{Laser}} = 50$ μW). RILS signals fade out with increasing temperature and at 10 K only a weak signal superimposed by emission background remains.

To conclude, we establish that low-temperature RILS experiments on collective "single-particle-like" [29,31,37] IMBE on twisted WSe_2 bilayers is a powerful method to experimentally study the moiré band formation selectively at the VBM around the K/K' states, their energetic separation and twist angle dependence providing a promising approach to study the band structure of twisted TMDCs at twist angles where correlation physics play an important role [3,12,13,16–18]. In agreement with theory, we identify several IMBE for a 3° $tWSe_2$, while for an 8° $tWSe_2$ only one clear IMBE and presumably one collective intraband excitation is observable and none for natural bilayers. The observation of collective IMBE by RILS in a semiconducting vdW bilayer demonstrates the potential to access the collective low-lying excitation spectra as unique fingerprints of individual quantum phases by RILS similar to correlated phases, e.g., in the fractional quantum Hall effect regime [45–47].

Acknowledgments—The authors gratefully acknowledge the German Science Foundation (DFG) for financial support via Grants No. WU 637/7-1 and No. WE 5342/5-1, and the Priority Program SPP 2244 "2DMP"—443273985, 443274199, as well as the computing time granted through JARA on the supercomputer JURECA [48] at Forschungszentrum Jülich. L. K. acknowledges support from the DFG through FOR 5249 (QUAST, Project No. 449872909). T. W. acknowledges support by the Cluster of Excellence "CUI: Advanced Imaging of Matter" of the DFG (EXC 2056, Project ID No. 390715994).

D. M. K. acknowledges support by the Deutsche Forschungsgemeinschaft (DFG, German Research Foundation) under Germany's Excellence Strategy—Cluster of Excellence Matter and Light for Quantum Computing (ML4Q) EXC 2004/1–390534769. We acknowledge support by the Max Planck–New York City Center for Nonequilibrium Quantum Phenomena.

[1] D. M. Kennes, M. Claassen, L. Xian, A. Georges, A. J. Millis, J. Hone, C. R. Dean, D. N. Basov, A. N. Pasupathy, and A. Rubio, Moiré heterostructures as a condensed-matter quantum simulator, Nat. Phys. **17**, 155 (2021).

[2] Y. Tang, L. Li, T. Li, Y. Xu, S. Liu, K. Barmak, K. Watanabe, T. Taniguchi, A. H. MacDonald, J. Shan, and K. F. Mak, Simulation of Hubbard model physics in WSe_2/Ws_2 moiré superlattices, Nature (London) **579**, 353 (2020).

[3] F. Wu, T. Lovorn, E. Tutuc, and A. H. MacDonald, Hubbard model physics in transition metal dichalcogenide moiré bands, Phys. Rev. Lett. **121**, 026402 (2018).

[4] L. Balents, C. R. Dean, D. K. Efetov, and A. F. Young, Superconductivity and strong correlations in moiré flat bands, Nat. Phys. **16**, 725 (2020).

[5] P. A. Pantaleón, A. Jimeno-Pozo, H. Sainz-Cruz, V. T. Phong, T. Cea, and F. Guinea, Superconductivity and correlated phases in non-twisted bilayer and trilayer graphene, Nat. Rev. Phys. **5**, 304 (2023).

[6] Y. Cao, V. Fatemi, S. Fang, K. Watanabe, T. Taniguchi, E. Kaxiras, and P. Jarillo-Herrero, Unconventional superconductivity in magic-angle graphene superlattices, Nature (London) **556**, 43 (2018).

[7] Y. Cao, V. Fatemi, A. Demir, S. Fang, S. L. Tomarken, J. Y. Luo, J. D. Sanchez-Yamagishi, K. Watanabe, T. Taniguchi, E. Kaxiras, R. C. Ashoori, and P. Jarillo-Herrero, Correlated insulator behaviour at half-filling in magic-angle graphene superlattices, Nature (London) **556**, 80 (2018).

[8] Z. Hao, A. M. Zimmerman, P. Ledwith, E. Khalaf, D. H. Najafabadi, K. Watanabe, T. Taniguchi, A. Vishwanath, and P. Kim, Electric field–tunable superconductivity in alternating-twist magic-angle trilayer graphene, Science **371**, 1133 (2021).

[9] J. M. Park, Y. Cao, K. Watanabe, T. Taniguchi, and P. Jarillo-Herrero, Tunable strongly coupled superconductivity in magic-angle twisted trilayer graphene, Nature (London) **590**, 249 (2021).

[10] Y. Zhang, R. Polski, C. Lewandowski, A. Thomson, Y. Peng, Y. Choi, H. Kim, K. Watanabe, T. Taniguchi, J. Alicea, F. von Oppen, G. Refael, and S. Nadj-Perge, Promotion of superconductivity in magic-angle graphene multilayers, Science **377**, 1538 (2022).

[11] F. Wu, T. Lovorn, E. Tutuc, I. Martin, and A. H. MacDonald, Topological insulators in twisted transition metal dichalcogenide homobilayers, Phys. Rev. Lett. **122**, 086402 (2019).

[12] J. Zang, J. Wang, J. Cano, and A. J. Millis, Hartree-Fock study of the moiré Hubbard model for twisted bilayer transition metal dichalcogenides, Phys. Rev. B **104**, 075150 (2021).

[13] L. Xian, M. Claassen, D. Kiese, M. M. Scherer, S. Trebst, D. M. Kennes, and A. Rubio, Realization of nearly dispersionless bands with strong orbital anisotropy from destructive interference in twisted bilayer MoS_2, Nat. Commun. **12**, 5644 (2021).

[14] L. Wang, E.-M. Shih, A. Ghiotto, L. Xian, D. A. Rhodes, C. Tan, M. Claassen, D. M. Kennes, Y. Bai, B. Kim, K. Watanabe, T. Taniguchi, X. Zhu, J. Hone, A. Rubio, A. N. Pasupathy, and C. R. Dean, Correlated electronic phases in twisted bilayer transition metal dichalcogenides, Nat. Mater. **19**, 861 (2020).

[15] A. Ghiotto, E.-M. Shih, G. S. S. G. Pereira, D. A. Rhodes, B. Kim, J. Zang, A. J. Millis, K. Watanabe, T. Taniguchi, J. C. Hone, L. Wang, C. R. Dean, and A. N. Pasupathy, Quantum criticality in twisted transition metal dichalcogenides, Nature (London) **597**, 345 (2021).

[16] S. Ryee and T. O. Wehling, Switching between Mott-Hubbard and Hund physics in moiré quantum simulators, Nano Lett. **23**, 573 (2023).

[17] L. Klebl, A. Fischer, L. Classen, M. M. Scherer, and D. M. Kennes, Competition of density waves and superconductivity in twisted tungsten diselenide, Phys. Rev. Res. **5**, L012034 (2023).

[18] Y.-M. Wu, Z. Wu, and H. Yao, Pair-density-wave and chiral superconductivity in twisted bilayer transition metal dichalcogenides, Phys. Rev. Lett. **130**, 126001 (2023).

[19] Z. Wang, Y.-H. Chiu, K. Honz, K. F. Mak, and J. Shan, Electrical tuning of interlayer exciton gases in WSe_2 bilayers, Nano Lett. **18**, 137 (2018).

[20] D. Halbertal *et al.*, Moiré metrology of energy landscapes in Van der Waals heterostructures, Nat. Commun. **12**, 242 (2021).

[21] T. I. Andersen, G. Scuri, A. Sushko, K. De Greve, J. Sung, Y. Zhou, D. S. Wild, R. J. Gelly, H. Heo, D. Bérubé, A. Y. Joe, L. A. Jauregui, K. Watanabe, T. Taniguchi, P. Kim, H. Park, and M. D. Lukin, Excitons in a reconstructed moiré potential in twisted WSe_2/WSe_2 homobilayers, Nat. Mater. **20**, 480 (2021).

[22] E. Li, J.-X. Hu, X. Feng, Z. Zhou, L. An, K. T. Law, N. Wang, and N. Lin, Lattice reconstruction induced multiple ultra-flat bands in twisted bilayer WSe_2, Nat. Commun. **12**, 5601 (2021).

[23] S. Zhao, Z. Li, X. Huang, A. Rupp, J. Göser, I. A. Vovk, S. Y. Kruchinin, K. Watanabe, T. Taniguchi, I. Bilgin, A. S. Baimuratov, and A. Högele, Excitons in mesoscopically reconstructed moiré heterostructures, Nat. Nanotechnol. **18**, 572 (2023).

[24] M. Troue, J. Figueiredo, L. Sigl, C. Paspalides, M. Katzer, T. Taniguchi, K. Watanabe, M. Selig, A. Knorr, U. Wurstbauer, and A. W. Holleitner, Extended spatial coherence of interlayer excitons in $MoSe_2/WSe_2$ heterobilayers, Phys. Rev. Lett. **131**, 036902 (2023).

[25] O. Karni *et al.*, Structure of the moiré exciton captured by imaging its electron and hole, Nature (London) **603**, 247 (2022).

[26] A. Sood, J. B. Haber, J. Carlström, E. A. Peterson, E. Barre, J. D. Georgaras, A. H. M. Reid, X. Shen, M. E. Zajac, E. C. Regan, J. Yang, T. Taniguchi, K. Watanabe,

F. Wang, X. Wang, J. B. Neaton, T. F. Heinz, A. M. Lindenberg, F. H. da Jornada, and A. Raja, Bidirectional phonon emission in two-dimensional heterostructures triggered by ultrafast charge transfer, Nat. Nanotechnol. **18**, 29 (2023).

[27] Z. Zhang, Y. Wang, K. Watanabe, T. Taniguchi, K. Ueno, E. Tutuc, and B. J. LeRoy, Flat bands in twisted bilayer transition metal dichalcogenides, Nat. Phys. **16**, 1093 (2020).

[28] G. Gatti, J. Issing, L. Rademaker, F. Margot, T. A. de Jong, S. J. van der Molen, J. Teyssier, T. K. Kim, M. D. Watson, C. Cacho, P. Dudin, J. Avila, K. C. Edwards, P. Paruch, N. Ubrig, I. Gutiérrez-Lezama, A. F. Morpurgo, A. Tamai, and F. Baumberger, Flat Γ moiré bands in twisted bilayer WSe_2, Phys. Rev. Lett. **131**, 046401 (2023).

[29] A. Pinczuk, L. Brillson, E. Burstein, and E. Anastassakis, Resonant light scattering by single-particle electronic excitations in $n-$GaAs, Phys. Rev. Lett. **27**, 317 (1971).

[30] G. Abstreiter, T. Egeler, S. Beeck, A. Seilmeier, H. Hübner, G. Weimann, and W. Schlapp, Electronic excitations in narrow GaAs/AlGaAs quantum well structures, Surf. Sci. **196**, 613 (1988).

[31] S. Das Sarma and D.-W. Wang, Resonant raman scattering by elementary electronic excitations in semiconductor structures, Phys. Rev. Lett. **83**, 816 (1999).

[32] See Supplemental Material at http://link.aps.org/supplemental/10.1103/PhysRevLett.133.046902 for further information on experimental methods and procedures, on theoretical calculations as well as additional figures with supporting experimental and theoretical data sets, which includes Refs. [33–35].

[33] G. Scuri, T. I. Andersen, Y. Zhou, D. S. Wild, J. Sung, R. J. Gelly, D. Bérubé, H. Heo, L. Shao, A. Y. Joe, A. M. Mier Valdivia, T. Taniguchi, K. Watanabe, M. Lončar, P. Kim, M. D. Lukin, and H. Park, Electrically tunable valley dynamics in twisted WSe_2/WSe_2 bilayers, Phys. Rev. Lett. **124**, 217403 (2020).

[34] F. Sigger, H. Lambers, K. Nisi, J. Klein, N. Saigal, A. W. Holleitner, and U. Wurstbauer, Spectroscopic imaging ellipsometry of two-dimensional TMDC heterostructures, Appl. Phys. Lett. **121**, 071102 (2022).

[35] J. P. Bange, P. Werner, D. Schmitt, W. Bennecke, G. Meneghini, A. AlMutairi, M. Merboldt, K. Watanabe, T. Taniguchi, S. Steil, D. Steil, R. T. Weitz, S. Hofmann, G. S. M. Jansen, S. Brem, E. Malic, M. Reutzel, and S. Mathias, Ultrafast dynamics of bright and dark excitons in monolayer WSe_2 and heterobilayer WSe_2/MoS_2, 2D Mater. **10**, 035039 (2023).

[36] G. Abstreiter and K. Ploog, Inelastic light scattering from a quasi-two-dimensional electron system in GaAs-$Al_xGa_{1-x}As$ heterojunctions, Phys. Rev. Lett. **42**, 1308 (1979).

[37] S. Meier, Paulo E. Faria Junior, F. Haas, E.-S. Heller, F. Dirnberger, V. Zeller, T. Korn, J. Fabian, D. Bougeard, and C. Schüller, Intersubband excitations in ultrathin core-shell nanowires in the one-dimensional quantum limit probed by resonant inelastic light scattering, Phys. Rev. B **104**, 235307 (2021).

[38] L. P. McDonnell, J. J. S. Viner, P. Rivera, X. Xu, and D. C. Smith, Observation of intravalley phonon scattering of 2s excitons in $MoSe_2$ and WSe_2 monolayers, 2D Mater. **7**, 045008 (2020).

[39] H. Pan, F. Wu, and S. Das Sarma, Band topology, Hubbard model, Heisenberg model, and Dzyaloshinskii-Moriya interaction in twisted bilayer WSe_2, Phys. Rev. Res. **2**, 033087 (2020).

[40] T. Devakul, V. Crépel, Y. Zhang, and L. Fu, Magic in twisted transition metal dichalcogenide bilayers, Nat. Commun. **12**, 6730 (2021).

[41] S. Ryee and T. O. Wehling, Switching between Mott-Hubbard and Hund physics in moiré quantum simulators, Nano Lett. **23**, 573 (2023).

[42] S. Brem, K.-Q. Lin, R. Gillen, J. M. Bauer, J. Maultzsch, J. M. Lupton, and E. Malic, Hybridized intervalley moiré excitons and flat bands in twisted WSe_2 bilayers, Nanoscale **12**, 11088 (2020).

[43] U. Wurstbauer, D. Majumder, S. S. Mandal, I. Dujovne, T. D. Rhone, B. S. Dennis, A. F. Rigosi, J. K. Jain, A. Pinczuk, K. W. West, and L. N. Pfeiffer, Observation of nonconventional spin waves in composite-fermion ferromagnets, Phys. Rev. Lett. **107**, 066804 (2011).

[44] A. Kormányos, G. Burkard, M. Gmitra, J. Fabian, V. Zólyomi, N. D. Drummond, and V. Fal'ko, Corrigendum: k.p theory for two-dimensional transition metal dichalcogenide semiconductors (2015 2d mater. 2 022001), 2D Mater. **2**, 049501 (2015).

[45] U. Wurstbauer, K. W. West, L. N. Pfeiffer, and A. Pinczuk, Resonant inelastic light scattering investigation of low-lying gapped excitations in the quantum fluid at $\nu=5/2$, Phys. Rev. Lett. **110**, 026801 (2013).

[46] L. Du, U. Wurstbauer, K. W. West, L. N. Pfeiffer, S. Fallahi, G. C. Gardner, M. J. Manfra, and A. Pinczuk, Observation of new plasmons in the fractional quantum Hall effect: Interplay of topological and nematic orders, Sci. Adv. **5**, eaav3407 (2019).

[47] J. Liang, Z. Liu, Z. Yang, Y. Huang, U. Wurstbauer, C. R. Dean, K. W. West, L. N. Pfeiffer, L. Du, and A. Pinczuk, Evidence for chiral graviton modes in fractional quantum Hall liquids, Nature (London) **628**, 78 (2024).

[48] Jülich Supercomputing Centre, JURECA: Data centric and booster modules implementing the modular supercomputing architecture at Jülich Supercomputing Centre, J. Large-Scale Res. Facil. **7**, A182 (2021).